Preparation And Application of Carbon Aerogel/Cobalt Phosphate Composite for Desalination by Hybrid Capacitive Deionization Method

Beke, Michael Abraham
beke.michael@gmail.com, +2348083411699.
DOI: 10.56201/ijccp.vol.11.no2.2025.pg78.89

Abstract
The availability of freshwater remains a global challenge. But the abundant saline water from the sea and estuaries can be harnessed for the production of freshwater by desalination. Hence there is a pressing need to develop a cost-effective and dependable desalination technology. In this study, we investigate the application of carbon aerogel cobalt phosphate composite for desalination of saline water by the hybrid capacitive deionization method. Aerogel was prepared by the sol-gel method, the aerogel was then heated to 1000ºC under nitrogen gas flow to give carbon aerogel (CA). The CA was impregnated with cobalt and phosphate to give the composite [CA/$Co_3(PO_4)_2$]. From the cyclic voltammetry analysis, the specific capacitance of the CA is 191F/g while that of the composite is 750F/g. The galvanostatic charge/discharge test of the composite shows a capacitance retention of 99% after 2000 cycles of charge/discharge. The composite was applied as electrode material for desalination of 1000 mg/L, 2000 mg/L and 3000mg/L saline solutions separately by hybrid capacitive deionization at an applied potential of 2.0V. The desalination results shows that the salt adsorption of the electrode at 1000 mg/L, was 76 mg/g, at 2000 mg/L it was 112 mg/g, and at 3000 mg/L it was 157 mg/g. From the results, it is clear that the composite material will perform very well when used as electrode in building a HCDI equipment for commercial use.

Key words: *Carbon aerogel, Cobalt Phosphate, Hybrid Capacitive Deionization, Desalination*

1. Introduction

We live in a world where the demand for freshwater is always on the increase[1]. Hence new and innovative methods of freshwater production is essential to meet up with the demand for freshwater[2,3]. Desalination of the abundant saline water in the ocean and estuaries is one of such innovative methods for freshwater production. Developing a cost-effective and dependable desalination technology is key towards achieving this feat. Hence there has been much research lately in this field. Different desalination technologies have been developed over the decades[4–6], these are: thermal methods, osmotic methods, Electrodialysis, and Capacitive Deionization method. Among these methods, capacitive deionization (CDI) has gained much attention due to its low operational cost and dependability. CDI technology works by removing charged particles from a medium by electrically charge electrodes. The success of CDI for desalination depends on the nature of the electrode used[7,8]. When carbon materials are used as electrodes, it is called CDI technology, but when the carbon electrodes are electrochemically enhanced or completely replaced with other materials, it is called hybrid capacitive deionization (HCDI). In this study, carbon aerogel is used as the base electrode, it was then modified with cobalt phosphate. The resultant composite material (carbon aerogel cobalt phosphate) was then applied as electrode material for HCDI desalination study. The choice of these materials is based on previously reported performance of carbon aerogel (CA), Co, and Phosphates in HCDI desalination. M. Beke et al.[9], Applied a carbon aerogel polypyrrole (CA-PPy) composite for HCDI desalination, and a salt adsorption of 15.7 mg/g

was reported for the desalination of 800 mg/L saline solution. Also, the specific capacitance of the CA reported was 115F/g while that of the CA-PPy was 360F/g. Also, H. Zhou et al.[10], used a cellulose CA-PPy composite for energy storage material (supercapacitor) study. The composite was reported to have an electrical capacitance of 387.6 F/g and after a galvanostatic charge/discharge test of 10,000 cycles the composite was reported to have a capacitance retention of 92.7%. The result shows the composite has potentials as electrode material for HCDI desalination. Cobalt and phosphates are widely applied as battery materials[11]. They are reported to have Faradaic behaviour which enhance energy storage and charge transfer[12–14]. Cao. et al [11] applied Na3V2(PO4)3@C as electrode for HCDI desalination. An impressive ion adsorption value of 137.2 mg/g at an applied potential of 1.0V was reported. Hence the application of the adopted electrode material should perform very well in HCDI desalination.

2. Materials and Methods

Materials:

Resorcinol, Formaldehyde, Cobalt nitrate hexahydrate [$Co(NO_3)_2.6H_2O$], Phosphoric acid (H_3PO_4), Sodium chloride, Ethanol, Deionized water, Hydrochloric acid.

All the materials are used as purchased from the vendors.

2.1 Synthesis of Carbon Aerogel (CA).

The synthesis of CA started with the preparation of aerogel by the sol–gel condensation of formaldehyde and resorcinol. 0.45g of resorcinol was dissolved in 20mL of acetonitrile, 0.63mL of formaldehyde was added, followed by 0.06mL of concentrated hydrochloric acid as catalyst; the mixture was stirred for 5min. The solution was then transferred into 50mL centrifuge tubes and left to age for three days. The sol–gel was then frozen to -80ºC, after which it was freeze-dried to form the aerogel. The aerogel was then carbonised in a tube furnace at 1000ºC for 4hrs. under nitrogen gas flow to give CA.

2.2 Synthesis of Carbon Aerogel/Cobalt Phosphate Composite [CA/$Co_3(PO_4)_2$].

$Co(NO_3)_2.6H_2O$ and H_3PO_4 were dissolved in ethanol solution in a 1:2 molar ratio. A 1.0 molar portion of the CA was measured and added into the precursor solution; this was then sonicated for 10 hours. The resultant composite was filtered off, washed with ethanol and dried. The composite was then heated to 300ºC under nitrogen gas. This converts the cobalt phosphate in the composite into nano size particles.

3. Characterization

3.1 FTIR SPECTROSCOPY

FTIR spectroscopy was employed to investigate the functional groups in the materials prepared. The spectrum gave a broad absorption band at ~3400 cm^{-1} this indicate the presence of –OH on the surface of the material[15,16], while the band observed at ~1630 cm^{-1} is associated with aromatic (-C=C-) specie[17,18], and the cobalt and phosphate groups band are observed at ~1040 and 560 cm^{-1}[19,20]. These observations shows that the composite material was successfully synthesized. Figure 1, is the FTIR spectrum of the composite.

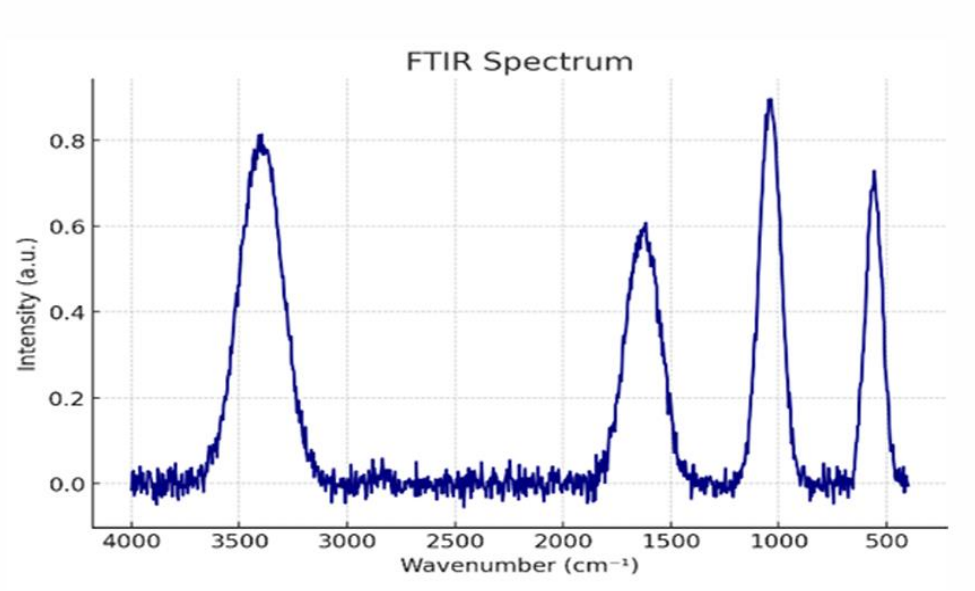

Figure 1. FTIR spectrum of composite.

3.2 X-RAY DIFFRACTION (XRD) Analysis

The crystalline nature of the material was analysed by XRD. The peaks observed at (16.5°, 25.2°, 31.3°, 36.8°) are crystalline peaks of $Co_3(PO_4)_2$[9,21], while the peak at ~24° indicates the presence of amorphous carbon [21,22]. Figure 2, shows the XRD pattern of the composite.

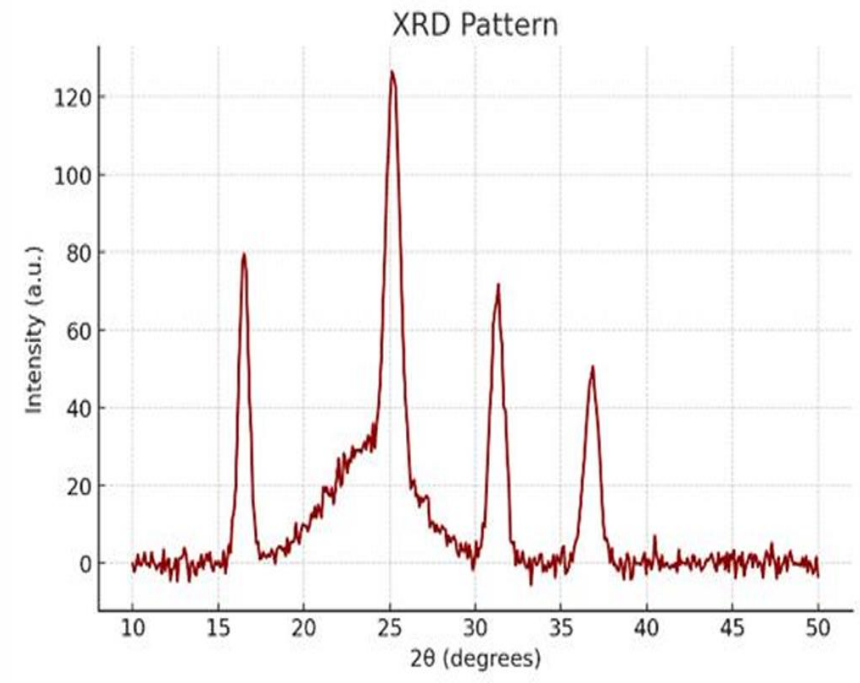

Figure 2. XRD of Composite.

3.3 Scanning Electron Microscopy (SEM) and Transmission Electron Microscopy (TEM) Analysis

SEM and TEM were used to analyse the microstructure of the materials. The SEM image shows that the CA have a porous sponge-like structure which indicates the presence of a well-developed CA structure that can support the cobalt phosphate[23,24]. This

morphology allows ion accessibility. Figure 3(A), is the SEM image of the composite. The TEM image is shown in Figure 3(B). It reveals the composite exist as nano particles and they are dispersed within the CA matrix. The bright and dark patterns oberved suggest a crystalline region that is consistent with cobalt phosphate materials[18,25–27].

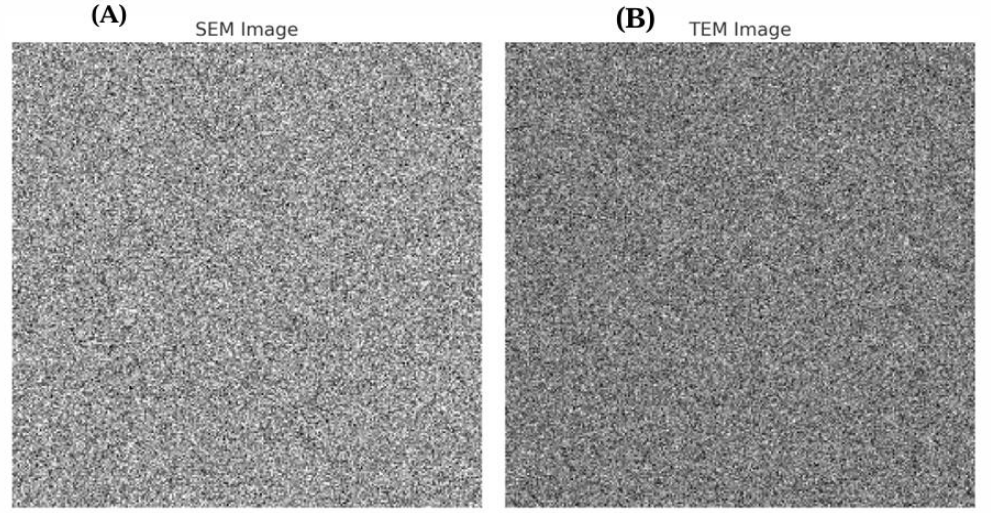

Figure 3. SEM and TEM images of Composite.

3.4 Brunauer-Emmett-Teller (BET) Analysis

The surface area and porosity of the material was analysed by N_2 adsorption /desorption measurements. The composite shows an IUPAC Type IV isotherm with a H3 hysteresis loop. The data obtained from the analysis confirms that the composite is mesoporous, which will facilitate rapid ion diffusion, ideal for supercapacitor application[9,28,29]. The values of the surface area, pore volume and average pore diameter are given in Table 1. The isotherm of the composite is shown in Figure 4.

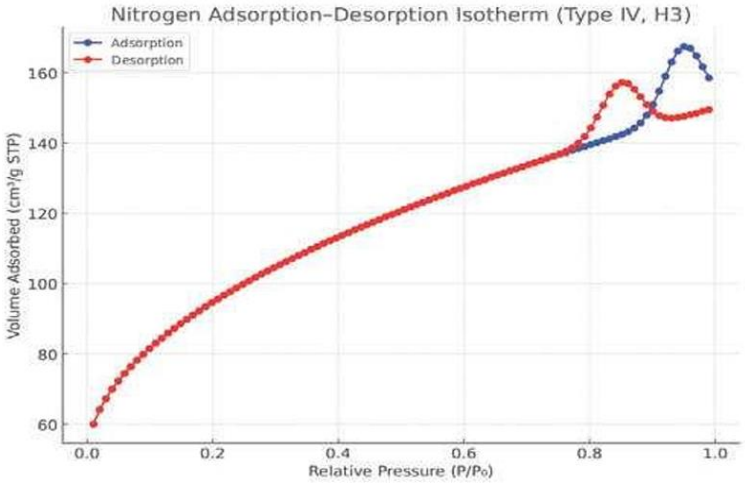

Figure 4. BET Isotherm of composite

Table 1. BET Surface Area Analysis Summary

Parameter	Value
Surface Area	520 m^2/g
Pore Volume	0.45 cm^3/g
Average Pore Diameter	4.8 nm

4 Electrochemical Analysis

The electrochemical properties of the materials were analysed by Cyclic voltammetry (CV) and Electrochemical Impedence spectroscopy (EIS).

4.1 Cyclic Voltammetry (CV)

The electrochemical tests were done using a Gamry electrochemical potentiostat work-station. A 1.0M KCl electrolyte was used and the applied potential window was (-0.3 to+0.3) V. The CV curve of CA shows a quasi-duck shape which is common with electric double layer capacitance (EDLC) behaviour. The slope and sinosoidial pattern suggest the presence of graphite in the CA. This will support some pseudocapacitance through REDOX reactions[25,26,30].

The duck shaped cyclogram of the composite is associated with Fadadaic behaviour, which will enhance the power and energy density of the material[28,31–33]. The specific capacitance of the CA is 191 F/g while that of the composite material is 750 F/g. The values of the specific capacitance were calculated from the data of the CV analysis. Imparatively, the addition of the cobalt phosphate to the CA enhanced the electrochemical properties of the composite as expected. It also means that the material will performance excellently when applied as electrode material for HCDI desalination[34–37].

The cyclogram of the CA and composite are shown in Figure 5.

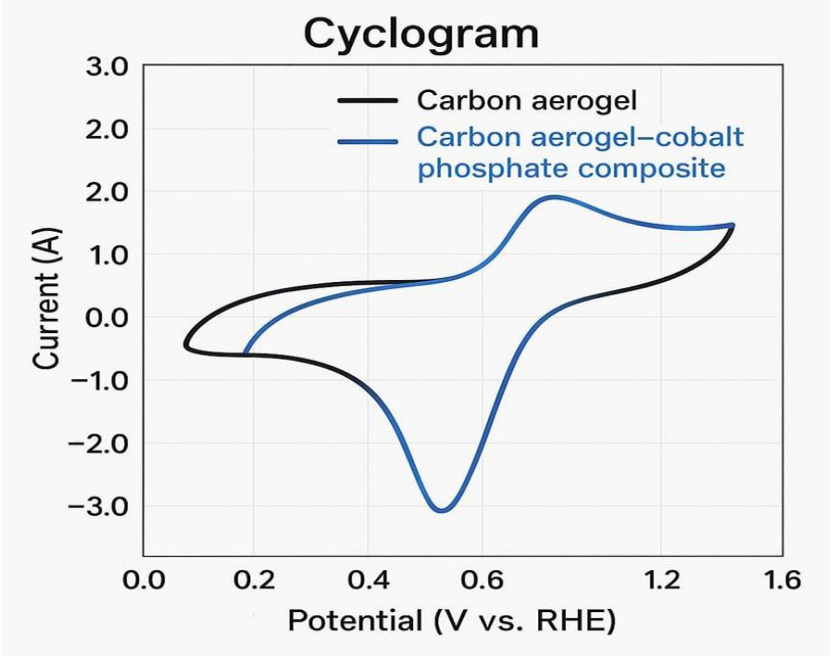

Figure 5, Cyclogram of CA and composite

4.2 Electrochemical Impedance Spectroscopy (EIS)

EIS was employed to study the charge transfer of the materials. The EIS was conducted using a three-electrode electrochemical work station. A 1.0 M KCl electrolyte was used, the applied potential was 0.22V and the frequency range is 10^5 Hz to 0.1 Hz. The EIS result shows that the charge resistance of CA is 199Ω while that of the composite is 100Ω. The Nyquist plot shows that the composite has a rapid charge transfer, which is demonstrated by the smaller semi-circle of the composite[38–40]. This supports the fact that the addition of the cobalt phosphate enhanced the electrochemical properties of the CA.

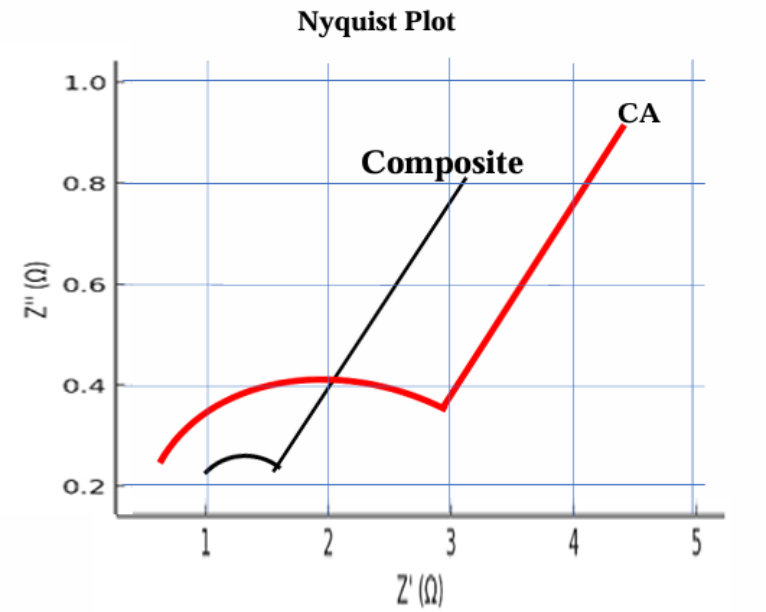

Figure 6, Nyquist plot of CA and Composite

5. Galvanostatic Charge/Discharge

Galvanostatic charge/discharge was used to investigate the electrochemical stability of the composite. The composite was stable over 2000 cycles of charge/discharge. The capacitance retention over the 2000 cycles was 99%. This means that the material can withstand 2000 cycles of usage and still maintain its electrochemical properties. Figure 7 shows a complete three cycles of charge/ discharge curve.

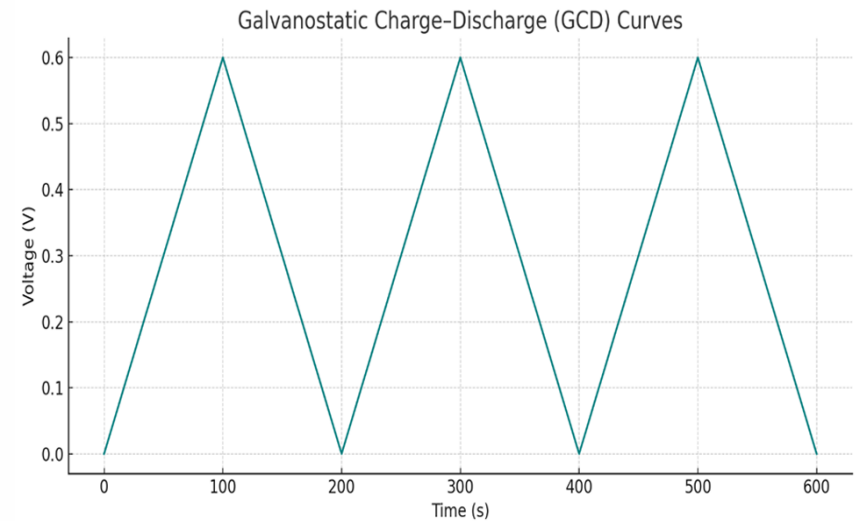

Figure 7, Galvanostatic charge/discharge curve.

6 DESALINATION EXPERIMENT

The desalination experiment was carried out in a batch mode using a CDI cell, as shown in Scheme 2. The cathode is activated carbon modified with the composite, while the anode is activated carbon. The electrodes are separated with a parafilm material, 1.5 cm apart in a 100 mL beaker containing 50 mL of NaCl solution. An electrical conductivity meter (abs) was used to measure the conductivity of the solution throughout the experiment. 1000 mg/L, 2000 mg/L, and 3000 mg/L concentrations of NaCl were used for this experiment. A direct current (DC) of 2.0 V was then applied to the CDI cell through the electrodes. The formula in equation 1. was used to determine the ion adsorption capacity (SAC) of the electrode.

$$SAC = \frac{\Delta C \times \Delta V(L)}{m} \quad (1)\ [41]$$

SAC = salt ion adsorption capacity, $\Delta\ C$ = Change in concentration of the saline solution, V = volume of saline solution, and m = mass of the composite on the electrode.

6.1 HCDI Desalination

Hybrid capacitive desalination experiment was done in a batch mode. 1000 mg/L, 2000 mg/L, and 3000 mg/L concentrations of NaCl solutions were used. At the start of the experiment, ion adsorption increases sharply from the conductivity meter reading, it gradually slowed until it stopped. The reduction in conductivity in the desalination experiment is indicative of ion adsorption. This demonstrates that the composite electrode material is electrochemically active and effective for HCDI desalination. It also proves that the desalination was successful. The desalination proceeds as the positive ions migrates to the negative electrode and negative ions to the positive electrode. The adsorbed ions were stored on and within the electric double layer (EDL) of the CA while it is stored by Faradaic intercalation in the cobalt phosphate within the composite electrode material until saturation is reached. The saturated electrodes were transferred into a beaker containing deionized water and the polarity of the applied potential reversed for desorption of the ions loaded on the electrodes. The desorbed electrodes are rinsed with deionized water and the desalination is repeated until the desired concentration of dissolved salt is reached. For freshwater, the concentration of total dissolved salt is about 500mg/L For deionized water all the dissolved ions need to be removed. The results of the desalination shows that the SAC at 1000mg/L is 76mg/g, at 2000mg/L the SAC is 112mg/g, and at 3000mg/L the SAC is 157mg/g. Table 2 shows the results and relevant data of the desalination.

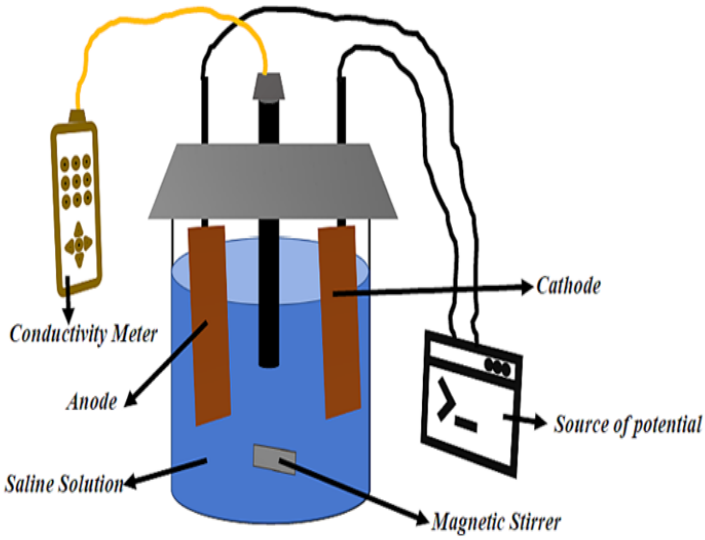

Scheme 1. Schematic of HCDI Desalination[41]

Table 2, HCDI Desalination Data.

Conc. of NaCl (mg/L)	Desalination time (min)	Initial Conc. mg/L	Final Conc. mg/L	Mass of Composite (m)	Volume of NaCl (L)	Salt Adsorp. Cap. (mg/g)
1000	**350**	**995**	**159**	**0.55**	**0.05**	**76**
2000	**310**	**1991**	**714.2**	**0.57**	**0.05**	**112**
3000	**260**	**2988**	**1198.2**	**0.57**	**0.05**	**157**

Comparing Results

The results of this study shows that the electrode material adopted performed better than most of the previous electrode materials used for HCDI desalination study as could be seen in Table 3.

Table 3, Results compared with that previously reported.

s/n	Electrode Mat.	Specific Capac(F/g)	Applied Volt(V)	SAC (mg/g)	Reference
1	CA	141	1.2	5.27	[21]
2	A-NiO	46.53	1.2	7.46	[42]
3	CA	156	1.2	29.7	[43]
4	CA-PPy	360	1.2	15.7	[9]
5	$Na_3V_2(PO_4)_3$@C	----	1.0	137.2	[11]
6	CA/$Co_3(PO_4)_2$	750	1.2	157	Current Study

7 Conclusion

The composite material CA/$Co_3(PO_4)_2$ was successfully prepared and its properties analysed. The results show that the composite has both electric double layer capacitance (because of the CA) and pseudocapacitance due to the presence of the cobalt phosphate. The specific capacitance of the composite from the CV analysis is 750 F/g. The electrochemical stability analysis shows that the material is stable over 2000 cycles of charge/discharge. The results of the HCDI desalination shows that the salt adsorption capacity of the composite at 1000 mg/L of saline solution is 76 mg/g, at 2000 mg/L is 112 mg/g, and at 3000 mg/L is 157 mg/g. The

results show that the composite performed better than previously reported carbon aerogel composite materials. This research further consolidates on the claim by Cao J. et al (2019) and other researcher with similar remarks that the application of Faradaic electrode materials as electrodes in HCDI desalination will overcome the limitations observed with carbon-based electrodes by improving their electrochemical properties and ion adsorption capacity.

Funding: This research is funded by the author
Conflict of interest: The author declares that there is no conflict of interest

Reference

[1] K.C. Ng, K. Thu, Y. Kim, A. Chakraborty, G. Amy, Adsorption desalination: An emerging low-cost thermal desalination method, Desalination 308 (2013) 161–179. https://doi.org/10.1016/j.desal.2012.07.030.

[2] Y.H. Teow, A.W. Mohammad, New generation nanomaterials for water desalination: A review, Desalination 451 (2019) 2–17. https://doi.org/10.1016/J.DESAL.2017.11.041.

[3] J.L. Prante, J.A. Ruskowitz, A.E. Childress, A. Achilli, RO-PRO desalination: An integrated low-energy approach to seawater desalination, Appl Energy 120 (2014) 104–114. https://doi.org/10.1016/j.apenergy.2014.01.013.

[4] M.A. Alaei Shahmirzadi, S.S. Hosseini, J. Luo, I. Ortiz, Significance, evolution and recent advances in adsorption technology, materials and processes for desalination, water softening and salt removal, J Environ Manage 215 (2018) 324–344. https://doi.org/10.1016/j.jenvman.2018.03.040.

[5] A.N. Mabrouk, H.E.S. Fath, Technoeconomic study of a novel integrated thermal MSF-MED desalination technology, Desalination 371 (2015) 115–125. https://doi.org/10.1016/j.desal.2015.05.025.

[6] T. Mezher, H. Fath, Z. Abbas, A. Khaled, Techno-economic assessment and environmental impacts of desalination technologies, (2010). https://doi.org/10.1016/j.desal.2010.08.035.

[7] X. Su, T.A. Hatton, Redox-electrodes for selective electrochemical separations, Adv Colloid Interface Sci 244 (2017) 6–20. https://doi.org/10.1016/j.cis.2016.09.001.

[8] R.B. Rakhi, W. Chen, H.N. Alshareef, Conducting polymer/carbon nanocoil composite electrodes for efficient supercapacitors, J Mater Chem 22 (2012) 5177–5183. https://doi.org/10.1039/C2JM15740C.

[9] M. Beke, T. Velempini, E. Prabakaran, K. Pillay, PREPARATION OF CARBON-AEROGEL POLYPYRROLE COMPOSITE FOR DESALINATION BY HYBRID CAPACITIVE DESALINATION METHOD, Arabian Journal of Chemistry (2022) 104412. https://doi.org/10.1016/j.arabjc.2022.104412.

[10] H. Zhuo, Y. Hu, Z. Chen, L. Zhong, Cellulose carbon aerogel/PPy composites for high-performance supercapacitor, Carbohydr Polym 215 (2019) 322–329. https://doi.org/10.1016/J.CARBPOL.2019.03.101.

[11] J. Cao, Y. Wang, L. Wang, F. Yu, J. Ma, Na(3)V(2)(PO(4))(3)@C as Faradaic Electrodes in Capacitive Deionization for High-Performance Desalination., Nano Lett 19 (2019) 823–828. https://doi.org/10.1021/acs.nanolett.8b04006.

[12] Q. Li, Y. Zheng, D. Xiao, T. Or, R. Gao, Z. Li, M. Feng, L. Shui, G. Zhou, X. Wang, Z. Chen, Faradaic Electrodes Open a New Era for Capacitive Deionization, (2020). https://doi.org/10.1002/advs.202002213.

[13] L. Guo, D. Kong, M.E. Pam, S. Huang, M. Ding, Y. Shang, C. Gu, Y. Huang, H.Y. Yang, The efficient faradaic Li4Ti5O12@C electrode exceeds the membrane capacitive desalination performance, J Mater Chem A Mater 7 (2019) 8912–8921. https://doi.org/10.1039/C9TA00700H.

[14] C. Zhang, D. He, J. Ma, W. Tang, T.D. Waite, Faradaic reactions in capacitive deionization (CDI) - problems and possibilities: A review, Water Res 128 (2018) 314–330. https://doi.org/10.1016/j.watres.2017.10.024.

[15] Q. Zhao, W. Wu, X. Wei, S. Jiang, T. Zhou, Q. Li, Q. Lu, Graphitic carbon nitride as electrode sensing material for tetrabromobisphenol-A determination, Sens Actuators B Chem 248 (2017) 673–681. https://doi.org/10.1016/j.snb.2017.04.002.

[16] P. Mary Rajaitha, K. Shamsa, C. Murugan, K.B. Bhojanaa, S. Ravichandran, K. Jothivenkatachalam, A. Pandikumar, Graphitic carbon nitride nanoplatelets incorporated titania based type-II heterostructure and its enhanced performance in

photoelectrocatalytic water splitting, SN Appl Sci 2 (2020). https://doi.org/10.1007/s42452-020-2190-9.

[17] N. Hebalkar, G. Arabale, S.R. Sainkar, S.D. Pradhan, I.S. Mulla, K. Vijayamohanan, P. Ayyub, S.K. Kulkarni, Study of correlation of structural and surface properties with electrochemical behaviour in carbon aerogels, n.d.

[18] T.C. Girija, M. V Sangaranarayanan, Polyaniline-based nickel electrodes for electrochemical supercapacitors—Influence of Triton X-100, J Power Sources 159 (2006) 1519–1526. https://doi.org/https://doi.org/10.1016/j.jpowsour.2005.11.078.

[19] M.A.E.P.J.H.M.J. Heslop, Preparation and structure characterization of carbons prepared from resorcinol-formaldehyde resin by CO2 activation Preparation and structure characterization of carbons prepared from resorcinol-formaldehyde resin by CO 2 activation, (2007). https://doi.org/10.1007/s10450-007-9065-x.

[20] Y. Wang, B. Chang, D. Guan, Mesoporous activated carbon spheres derived from resorcinol-formaldehyde resin with high performance for supercapacitors, (2015) 1783–1791. https://doi.org/10.1007/s10008-015-2789-8.

[21] Z. Cao, C. Zhang, Z. Yang, Q. Qin, Z. Zhang, X. Wang, J. Shen, Preparation of carbon aerogel electrode for electrosorption of copper ions in aqueous solution, Materials 12 (2019). https://doi.org/10.3390/ma12111864.

[22] E.O. Oseghe, S.O. Akpotu, E.T. Mombeshora, A.O. Oladipo, L.M. Ombaka, B.B. Maria, A.O. Idris, G. Mamba, L. Ndlwana, O.S. Ayanda, A.E. Ofomaja, V.O. Nyamori, U. Feleni, T.T.I. Nkambule, T.A.M. Msagati, B.B. Mamba, D.W. Bahnemann, Multi-dimensional applications of graphitic carbon nitride nanomaterials – A review, J Mol Liq 344 (2021) 117820. https://doi.org/10.1016/J.MOLLIQ.2021.117820.

[23] L. Xu, J. Zhang, J. Ding, T. Liu, G. Shi, X. Li, W. Dang, Y. Cheng, R. Guo, Pore structure and fractal characteristics of different shale lithofacies in the dalong formation in the western area of the lower yangtze platform, Minerals 10 (2020). https://doi.org/10.3390/min10010072.

[24] T. Gao, H. Li, F. Zhou, M. Gao, S. Liang, M. Luo, Mesoporous carbon derived from ZIF-8 for high efficient electrosorption, Desalination 451 (2019) 133–138. https://doi.org/10.1016/J.DESAL.2017.06.021.

[25] S. Porada, L. Borchardt, M. Oschatz, M. Bryjak, J.S. Atchison, K.J. Keesman, S. Kaskel, P.M. Biesheuvel, V. Presser, Direct prediction of the desalination performance of porous carbon electrodes for capacitive deionization, Energy Environ Sci 6 (2013) 3700–3712. https://doi.org/10.1039/c3ee42209g.

[26] S. Choi, B. Kim, J. Han, Integrated pretreatment and desalination by electrocoagulation (EC)–ion concentration polarization (ICP) hybrid, Lab Chip 17 (2017) 2076–2084. https://doi.org/10.1039/C7LC00258K.

[27] Y. Lu, X. Liu, W. Wang, J. Cheng, H. Yan, C. Tang, J.K. Kim, Y. Luo, Hierarchical, porous CuS microspheres integrated with carbon nanotubes for high-performance supercapacitors, Sci Rep 5 (2015). https://doi.org/10.1038/srep16584.

[28] A. Maghchiche, F.Z. Lakhal, A. Maghchiche, R. Nasri, A. Haouam, Composite Material Polystyrene Activated Carbon for Water Purification Extraction and characterization of polysaccharides from north Africa grass View project Use of plastic wastes for roads construction in Algeria View project Composite Material Polystyrene Activated Carbon for Water Purification, 2018. http://www.jmaterenvironsci.com.

[29] M. Zarei, Sensitive visible light-driven photoelectrochemical aptasensor for detection of tetracycline using ZrO2/g-C3N4 nanocomposite, Sensors International 1 (2020). https://doi.org/10.1016/j.sintl.2020.100029.

[30] H. Yamada, K. Yoshii, M. Asahi, M. Chiku, Y. Kitazumi, Cyclic Voltammetry Part 1: Fundamentals†, Electrochemistry 90 (2022). https://doi.org/10.5796/ELECTROCHEMISTRY.22-66082.
[31] P. Simon, Y. Gogotsi, Capacitive Energy Storage in Nanostructured Carbon–Electrolyte Systems, Acc Chem Res 46 (2013) 1094–1103. https://doi.org/10.1021/ar200306b.
[32] A. Mohammad, M.E. Khan, M.H. Cho, Sulfur-doped-graphitic-carbon nitride (S-g-C3N4) for low cost electrochemical sensing of hydrazine, J Alloys Compd 816 (2020). https://doi.org/10.1016/j.jallcom.2019.152522.
[33] P. Khajuria, R. Mahajan, S. Kumar, R. Prakash, Synthesis and optical properties of magnesium zirconium oxide, in: AIP Conf Proc, American Institute of Physics Inc., 2020. https://doi.org/10.1063/5.0001422.
[34] A. Bahloul, B. Nessark, E. Briot, H. Groult, A. Mauger, K. Zaghib, C.M. Julien, Polypyrrole-covered MnO2 as electrode material for supercapacitor, J Power Sources 240 (2013) 267–272. https://doi.org/10.1016/J.JPOWSOUR.2013.04.013.
[35] X. Li, X. Zhang, H. Li, Preparation and characterization of pyrrole/aniline copolymer nanofibrils using the template-synthesis method, J Appl Polym Sci 81 (2001) 3002–3007. https://doi.org/https://doi.org/10.1002/app.1750.
[36] L. Pan, H. Qiu, C. Dou, Y. Li, L. Pu, J. Xu, Y. Shi, Conducting polymer nanostructures: Template synthesis and applications in energy storage, Int J Mol Sci 11 (2010) 2636–2657. https://doi.org/10.3390/ijms11072636.
[37] M. Yu, J. Chen, J. Liu, S. Li, Y. Ma, J. Zhang, J. An, Mesoporous NiCo2O4 nanoneedles grown on 3D graphene-nickel foam for supercapacitor and methanol electro-oxidation, Electrochim Acta 151 (2015) 99–108. https://doi.org/10.1016/j.electacta.2014.10.156.
[38] H. Herrera Hernández, F. González Díaz, G.D.J. Fajardo San Miguel, J.C. Velázquez Altamirano, C.O. González Morán, J. Morales Hernández, Electrochemical Impedance Spectroscopy as a Practical Tool for Monitoring the Carbonation Process on Reinforced Concrete Structures, Arab J Sci Eng 44 (2019) 10087–10103. https://doi.org/10.1007/s13369-019-04041-z.
[39] N. Perez, Electrochemistry and Corrosion Science, 2016. https://doi.org/10.1007/978-3-319-24847-9.
[40] F. Mansfeld, H. Shih, H.J. Greene, C. Tsai, Analysis of EIS Data for Common Corrosion Processes, in: 1993. https://api.semanticscholar.org/CorpusID:137420955.
[41] M. Beke, T. Velempini, K. Pillay, Synthesis and application of NiO-ZrO2@g-C3N4 nanocomposite for high-performance hybrid capacitive deionisation, Results Chem 5 (2023). https://doi.org/10.1016/j.rechem.2023.100799.
[42] K.A. Gandionco, J.W. Kim, J.D. Ocon, J. Lee, Activated carbon-nickel (II) oxide electrodes for capacitive deionization process, Applied Chemistry for Engineering 31 (2020) 552–559. https://doi.org/10.14478/ace.2020.1064.
[43] Y. KL, Y. TY, S. Yiacoumi, C. Tsouris, V. ES, Electrosorption of ions from aqueous solutions by carbon aerogel: An electrical double-layer model, Langmuir 17 (2001) 1961–1969. https://doi.org/10.1021/la001527s.